

## DETECTION OF MASS LOSS FROM THE DWARF NOVA Z CAMELOPARDALIS

EDWARD L. ROBINSON\*

Department of Astronomy, University of Texas at Austin

*Received 1973 May 1*

### ABSTRACT

A series of image-tube spectra of the  $H\alpha$  emission line from the dwarf nova Z Cam has been acquired. The wings of the  $H\alpha$  profile have been used to obtain an improved orbital radial-velocity curve for the blue component of the binary system, and thus to obtain improved orbital elements. The center of the  $H\alpha$  profile displays a triple-peaked structure. This structure does not partake of the orbital radial-velocity variations of the underlying emission line, and must be formed in an expanding circum-system shell. The shell appears to be formed by continuous mass loss rather than by mass ejection during eruptions. A mass-loss rate greater than  $2.4 \times 10^{-9} M_{\odot} \text{ yr}^{-1}$  is deduced, which is probably sufficient to affect seriously the evolution of the Z Cam system.

*Subject headings:* dwarf novae — mass loss — stars, individual — U Geminorum stars

### I. INTRODUCTION

Z Camelopardalis is a dwarf nova. The mean time between its eruptions is 20 days, and during the eruptions its visual magnitude rises from about 14.0 to about 10.5 (e.g., Mayall 1965). Kraft, Krzeminski, and Mumford (1969, hereafter referred to as KKM) have shown that Z Cam is a close binary system with an orbital period of 0<sup>d</sup>289840. One of the stars is a main-sequence G1 star which fills its Roche lobe. The other star is a white dwarf (Robinson 1973*a*). According to KKM, the orbital inclination of Z Cam is limited to the range  $51^{\circ} < i < 66^{\circ}$ . There is a disk of gas rotating around the white dwarf which is maintained by matter transferred from the G star through the inner Lagrangian point. The strong, broad, and occasionally doubled emission lines of hydrogen, He I, and Ca II which are seen in the spectrum of Z Cam are formed in the disk of gas. As the transferred matter leaves the inner Lagrangian point, it is gravitationally accelerated, and becomes a high-velocity stream which penetrates through the outer layers of the disk of gas. When the stream penetrates to regions of sufficiently high density, a shock front forms and the kinetic energy of the stream is converted to light, creating an intense bright region, or spot. Except during eruptions, the bright spot contributes a minimum of 25 percent of the total light from Z Cam at optical wavelengths. The spot is unstable on time scales as short as 10 s, which produces the rapid flickering in the light curve of Z Cam (Robinson 1973*a*).

There is strong evidence that the white dwarf is the source of the eruptions in dwarf novae. Walker and Reagan (1971) show that in SS Cyg the erupting component has the same orbital motion as the white dwarf. White-dwarf pulsations appear in the dwarf novae during their eruptions (Warner and Robinson 1972; Robinson 1973*b*). The existence of the pulsations only during eruptions implies that the white dwarf is erupting. Also, broad hydrogen absorption lines appear in many dwarf novae during eruptions (e.g., Elvey and Babcock 1943). The breadth of these lines is difficult to explain except by pressure broadening at the surface of a degenerate star, and suggests that the white dwarf is the major source of luminosity during eruptions.

\* Present address: Lick Observatory, University of California, Santa Cruz.

TABLE 1  
JOURNAL OF OBSERVATIONS

Plate Number	JD <sub>⊙</sub> Mid-Exposure (2441300.0+)	Phase	$V(H\alpha)$ (km s <sup>-1</sup> )
U910.....	51.7135	0.527	- 74
U911.....	51.7593	0.685	+ 87
U912.....	51.8044	0.841	+ 60
U913.....	51.8537	0.011	+ 25
U915.....	52.7531	0.114	- 90
U916.....	52.8031	0.286	-208
U919.....	54.7531	0.014	- 10
U920.....	54.8003	0.177	-144
U921.....	54.8489	0.345	-173
U922.....	54.8947	0.503	-122
U926.....	55.6725	0.186	-105
U927.....	55.7156	0.335	-198
U928.....	55.7558	0.474	- 83
U929.....	55.7975	0.618	+ 11
U930.....	55.8385	0.759	+ 45
U931.....	55.8794	0.900	+ 69
U948*	72.6509	0.765	+ 77
U949*	72.6967	0.924	+ 81
U950*	72.7404	0.074	- 31

\* Contaminated by heavy image-tube fog.

On the basis of analogy to the classical novae, Gordelatse (1938) has calculated that the dwarf novae lose  $10^{-9} M_{\odot}$  per eruption. However, arguments by analogy cannot be considered meaningful, and there are positive grounds for believing that significant mass cannot be lost from the surface of the white dwarf during its eruptions. Walker and Chincarini (1968) show that the photosphere of the white dwarf expands at a rate of less than  $10 \text{ km s}^{-1}$  during eruptions. The observations of U Gem by Krzeminski (1965) as interpreted by Smak (1971) demonstrate that the disk of gas around the white dwarf does not suffer major disruption during eruptions. The existence, in many dwarf novae, of flickering during eruptions as well as during periods between eruptions (e.g., Robinson 1973*b*) also suggests that the disk is not disrupted. Therefore, the maximum expansion of the white dwarf during eruptions is limited to a small fraction of the radius of the disk.

In the paper we report spectroscopic observations of the  $H\alpha$  emission line in Z Cam. The observations are used to construct an improved radial-velocity curve for the emission lines. In addition, we find an expanding shell around Z Cam which is produced by mass loss. The mass is lost not from the surface of the white dwarf, but from the complex of gas surrounding the white dwarf. The rate of mass loss is probably sufficient to seriously affect the evolution of Z Cam.

## II. THE RADIAL-VELOCITY OBSERVATIONS

Spectra of Z Cam were obtained in 1972 February on the 82-inch (208-cm) telescope at McDonald Observatory using the ultraviolet image-tube spectrograph (UVITS) equipped with a single stage Westinghouse image tube, type WL-30677. All spectra covered the wavelength interval 5800–6800 Å at a dispersion of  $55 \text{ Å mm}^{-1}$  and were exposed for 55 minutes. The resolution of the plates is about  $45 \mu$ , or  $2.5 \text{ Å}$ . Each of the plates was traced with a  $20\text{-}\mu$  slit at  $5\text{-}\mu$  steps, using the Tull digital microphotometer, and converted to an intensity scale. The Tull microphotometer has a positioning accuracy of  $1 \mu$ , so that a wavelength calibration could be made for each tracing by

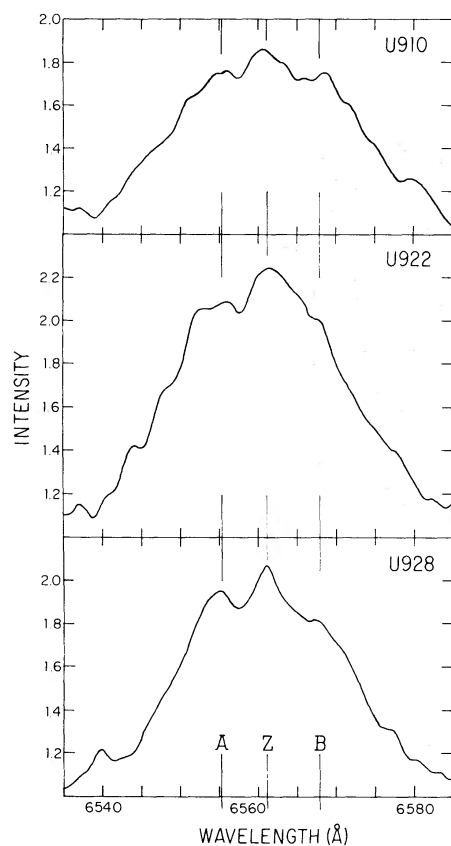


FIG. 1.—Profiles of  $H\alpha$  in Z Cam. The profiles are reduced to an intensity scale normalized to continuum = 1.00. The mean wavelengths of the A, B, and Z components of the fine structure are marked.

also tracing the comparison lines. The validity of this procedure was confirmed by measuring several of the plates on a standard cross-hair measuring engine. All wavelengths and velocities reported here were measured from these (digitized) tracings. The observations are summarized in table 1.

With the possible exception of the Na I D-lines, there are no absorption features in the spectra, and the only strong emission feature is the  $H\alpha$  emission line. Figure 1 shows

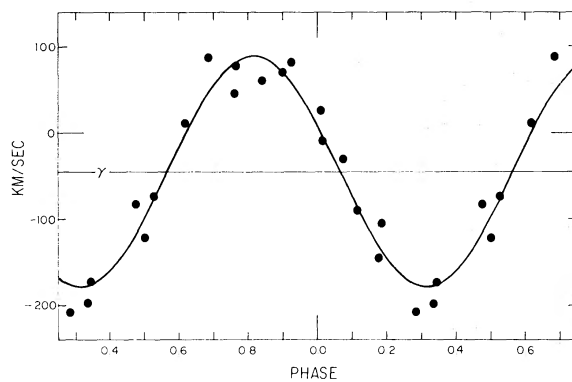


FIG. 2.—Radial-velocity curve of Z Cam as measured from the  $H\alpha$  emission line wings. The heavy curve is the least-squares fit of a circular orbit to the data.

TABLE 2

THE ORBITAL ELEMENTS OF Z CAMELOPARDALIS:

$$P = 0^{\text{d}}289840 \pm 0^{\text{d}}00001; T_0(\text{abs}) = \text{JD}_{\odot} 2438470.841 \pm 0.003;$$

$$e = 0 \text{ (assumed); } q = 1.41 \pm 0.15.$$

Element	G Star	White Dwarf
$\gamma$ (km s <sup>-1</sup> ).....	$-38 \pm 11$	$-45 \pm 6$
$K$ (km s <sup>-1</sup> ).....	$193 \pm 17$	$137 \pm 9$
$a \sin i$ (cm).....	$7.69 \times 10^{10} \pm 0.67$	$5.46 \times 10^{10} \pm 0.36$
$M \sin^3 i (M_{\odot})$ .....	$0.45 \pm 0.08$	$0.63 \pm 0.13$

the H $\alpha$  profile from three plates. The profiles have been smoothed to a 45- $\mu$  resolution using a running average digital filter. The center of the H $\alpha$  profile shows a multiple-peaked fine structure. Furthermore, large asymmetries appear in the H $\alpha$  profiles just after velocity maxima. These complexities are restricted to the central parts of the profile, so that reliable radial velocities were obtained by taking the mean of the velocities of the half-intensity points on the wings of the profiles. The resulting velocities are listed in table 1, and the radial velocity curve is shown in figure 2. The phases in figure 2 have been calculated from the orbital elements of KKM, in which zero phase is defined as inferior spectroscopic conjunction of the G star.

In calculating the orbit of Z Cam, we have adopted the position of KKM that the orbit of Z Cam is circular, but that gas streams may introduce a spurious phase lag into the emission-line radial velocities. The least-squares fit for a circular orbit is also shown in figure 2. The orbit from the H $\alpha$  lines lags behind the calculated phases by 0.065. This compares favorably with the lag of 0.059 found by KKM for the Ca II K-lines, so the orbital period found by KKM still provides a good fit to Z Cam. The phases listed in table 1 have been calculated using the period of KKM.

Our orbital elements do not differ significantly from those of KKM, but the formal errors of our elements are smaller. For completeness, then, we give in table 2 the revised elements, and their errors, calculated from our emission-line measurements, and the absorption-line measurements of KKM. The emission-line  $K$  term has been increased by 3 percent to correct for the effects of averaging the orbital velocity over the 55-minute exposures (Herbig 1960). The errors quoted in table 2 are the formal mean errors derived from the least-squares orbital solution, and do not reflect possible systematic errors. In particular, there may be errors due to distortion of the emission-line radial-velocity curve by bright spots (Smak 1970), and by noncircular motion in the disk (Paczynski, Piotrowski, and Turski 1968). Since the H $\alpha$  line profiles are well resolved, and since we have used the wings of the line, which are formed deep within the disk, we believe that the effects of both distortions have been minimized.

### III. OBSERVATIONAL EVIDENCE FOR MASS LOSS

The very fact that a radial-velocity curve could be constructed for Z Cam from the H $\alpha$  emission means that at least the wings and probably the bulk of the H $\alpha$  emission comes from the near vicinity of the white dwarf. This is not true for the fine structure near the line center. The fine structure remains stationary in wavelength while the underlying H $\alpha$  emission moves back and forth with orbital phase.

In preparation for identifying the fine structure, each profile was smoothed to a 45- $\mu$  resolution using a running mean filter. The smoothing considerably reduces plate noise in the profiles, particularly in the well-exposed regions near the line center. The wavelengths of all of the remaining fine-structure emission features, between the half-intensity points, have been measured on each of 16 spectra. The plates taken on JD

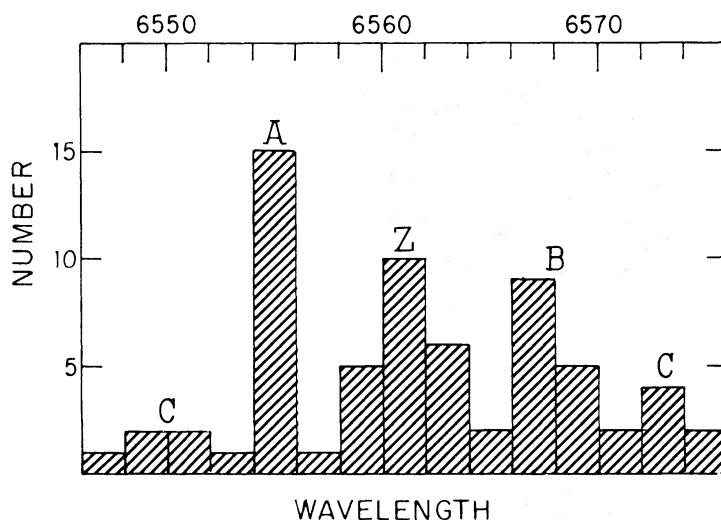


FIG. 3.—Histogram showing the distribution in wavelength of the fine-structure components of the  $H\alpha$  emission profile. Data from 16 plates have been combined in the histogram. The reality of the C components is not free from doubt.

2441372 have a high image-tube fog and were not used. The measured wavelengths on all 16 plates have been combined into a histogram giving the number of features in each  $2 \text{ \AA}$  interval. The histogram is shown in figure 3. At least a few of the measured features will be plate noise. Nevertheless, and in spite of the asymmetry of the underlying emission, a triple structure is evident. A feature appears between  $6554$  and  $6556 \text{ \AA}$  on every plate but one, and is labeled A. A weaker feature, displaced from the line center by an opposite and nearly equal amount to the A component, appears between  $6566$  and  $6570 \text{ \AA}$ , and has been labeled B. A broad, symmetrical peak in the histogram appears near the line center and has been labeled Z. The Z component is found on all but one plate, and is doubled on about half of the plates. In addition, a few emission features, labeled C, occasionally appear at large displacements from the line center. Although the reality of the C components is not free from doubt, their appearance is restricted to orbital phases just after the orbital velocity reaches a maximum. Since the  $H\alpha$  line profile is most asymmetrical at these phases, the C components may be reflecting substructure in the disk of gas around the white dwarf. In any case, the remaining discussion refers only to the A, B, and Z components whose reality is not in doubt. The triple-peaked structure is evident in the profiles shown in figure 1; the mean wavelengths of the three components are marked in the figure.

In figure 4 the wavelengths of the components have been plotted as a function of orbital phase. When more than one Z component has come from a single plate, they have been joined by a vertical bar. The three components clearly do not partake of the orbital radial-velocity variation of the underlying  $H\alpha$  emission line, which varies by nearly  $6 \text{ \AA}$  peak-to-peak. The wavelengths of the A component are randomly distributed in a band about  $2 \text{ \AA}$  wide with a mean wavelength of  $6555.2 \text{ \AA}$ . Although the B component appears to show coherent variations in wavelength, the total variation is only  $3 \text{ \AA}$ , and is out of phase with the orbital variation. Since the B component is weaker than the A component, its scatter may be attributed to measurement error, and it probably has a constant wavelength whose mean value is  $6567.4 \text{ \AA}$ . The scatter of the Z component is considerable, but if we use the average of the wavelengths of the two (or three, in one case) Z components when more than one appears, then the wavelengths of the Z component are also restricted to a band about  $2 \text{ \AA}$  wide, centered at

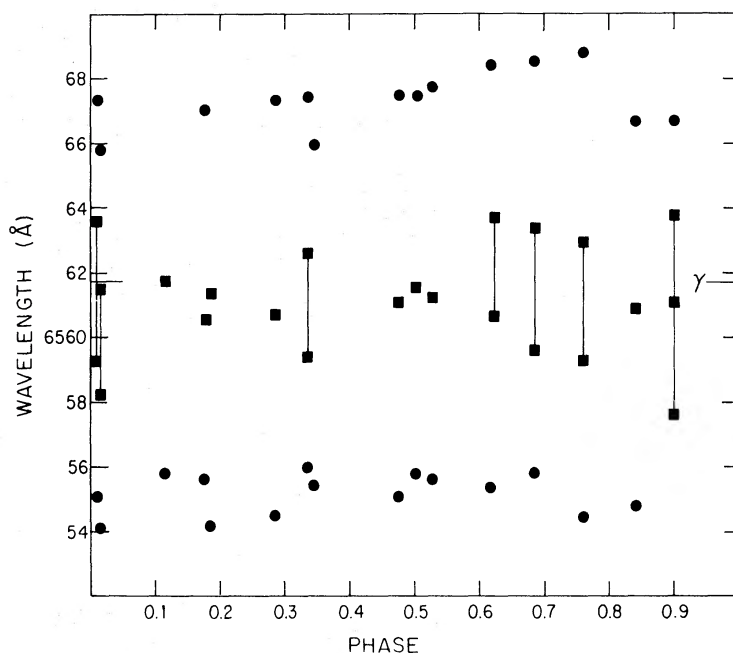


FIG. 4.—The distribution of the wavelengths of the fine-structure components of the  $H\alpha$  emission profile with orbital phase. The A and B components are marked with filled circles. The Z components are marked with filled squares. When more than one Z component has come from a single plate, they are joined by vertical straight lines. The three components do not show measurable variations in radial velocity with phase.

6561.1 Å. The triple-peaked system, while nearly symmetrical about the  $\gamma$ -velocity, is, in fact, displaced slightly to the blue by 0.5 Å.

Since the fine structure of the  $H\alpha$  emission line does not show orbital radial-velocity variations, it cannot be produced in the immediate vicinity of the stars, but must be produced by material outside the binary system. Insight into the structure of the material around Z Cam is gained by comparison to the classical novae. The emission lines which come from the shells ejected by the classical novae commonly have a multiple-peaked “castellated” structure (Payne-Gaposchkin 1957). The [O III]  $\lambda 4959$  emission line from CP Pup has a triple-peaked structure quite similar to that of Z Cam (Greenstein 1960). Hutchings (1972) has calculated the profiles to be expected from expanding shells with a variety of geometries and aspects. A reasonable estimate of the inclination of Z Cam is  $60^\circ$ . Figure 2 in Hutchings gives profiles for a variety of conical polar ejecta for an aspect of  $60^\circ$ . Most of the profiles bear a close resemblance to the  $H\alpha$  profiles of Z Cam. Indeed, for cone angle limits of  $60^\circ$  and  $70^\circ$ , the central peak of Hutchings’s profiles is weakly doubled, which may correspond to the doubling of the Z component of Z Cam. Hutchings notes that self-absorption reduces the redward side of the profile more than the blueward side. We may also expect self-absorption to produce the slight blueshift of the fine structure which we have observed. While other geometries are possible, the simplicity of the geometry of conical polar ejecta, and the completeness with which polar ejecta can reproduce the observed details of the  $H\alpha$  emission from Z Cam argue strongly that this geometry is correct. We note, however, that the geometry refers to the emission distribution, rather than the mass distribution. It may well be that the shell is nearly spherically symmetric, and that the mass in the plane of the orbit is not seen because of shadowing by the disk of ionizing radiation from near the center of the disk. For concreteness, we adopt a cone angle of  $60^\circ$ , which

gives an expansion velocity of one-half the separation of the A and B components, or  $V_E = 280 \text{ km s}^{-1}$ .

#### IV. THE MASS-LOSS MECHANISM

We have noted in the introduction that an abrupt ejection of mass of the type seen in the eruptions of the classical novae is unlikely to be occurring in the dwarf novae. Present evidence suggests that mass is lost more or less continuously from the gas structure in the Roche lobe surrounding white dwarf.

Smak (1969) and Huang (1972) have shown that the emission line profile produced by a rotating disk of gas is double-peaked, and that the positions of the peaks correspond closely to the projected rotational velocity of the outer edge of the disk. The higher members of the Balmer series of Z Cam occasionally show such a double-peaked profile (Kraft 1962, 1963). Kraft has kindly lent us his spectra of Z Cam for remeasurement. The spectra have been described in detail in KKM. Figure 5 gives the three profiles of  $H\delta$  from plate N2171. No density-intensity calibration is available, so the profiles have been left on a scale proportional to density. The orbital phase of each profile is also given in figure 5. The profiles are double-peaked, and—in marked contrast to the fine structure of the  $H\alpha$  profile—the double peaks of the  $H\delta$  profile show the same radial-velocity variations as the wings of the profile. Clearly the double peaks are produced by the disk of gas around the white dwarf. The mean separation of the peaks in the  $H\delta$  profiles is  $9.3 \text{ \AA}$ , or  $680 \text{ km s}^{-1}$ . The projected circular velocity of the outer edge of the disk is one-half the separation, or  $v \sin i = 340 \text{ km s}^{-1}$ . Assuming Keplerian motion in the disk, we have

$$\frac{r}{A} = \frac{GM_D \sin^3 i}{A \sin i (v \sin i)^2}, \quad (1)$$

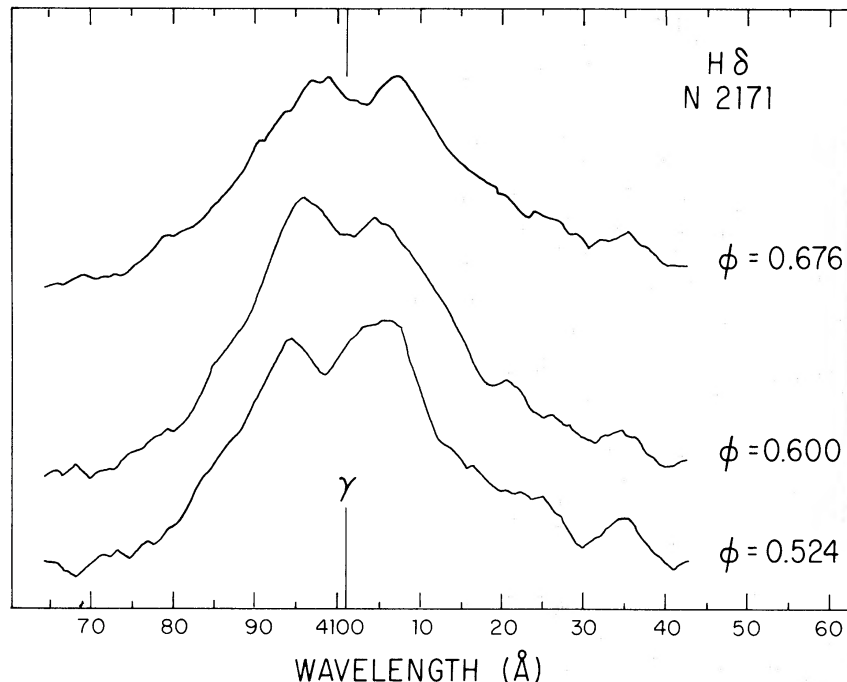


FIG. 5.—Profiles of  $H\delta$  in Z Cam from plate N2171 taken by Kraft (details given in KKM). The vertical scale is proportional to density. Both the double peak and the underlying  $H\delta$  emission show orbital radial-velocity variations and come from the vicinity of the white dwarf.

where  $r$  is the radius of the disk,  $A$  is the separation of the centers of mass of the stars, and  $G$  is the gravitational constant. Using the orbital elements given in table 1, we find  $r/A = 0.55$ . Since the mass ratio of Z Cam is near 1, the disk overfills the Roche lobe of the white dwarf. Using similar arguments, Walker and Chincarini (1968) find that the disk of gas in SS Cyg also overfills its Roche lobe. Since the outer edges of disks this near to the limits of their Roche lobes will not be in Keplerian motion, the disks in both systems probably fit within, but essentially fill their Roche lobes. The gas nearest the limits of the Roche lobe is very weakly bound to the white dwarf, and minor perturbations on the gas may cause extensive mass loss from the system.

The different behavior of the  $H\delta$  profile from the  $H\alpha$  profile of Z Cam requires that the Balmer decrement of the shell be much steeper than the Balmer decrement of the gas disk. The classical nova DQ Herculis shows a similar difference of decrements between its disk of gas and the shell ejected during its eruption, which results in a similar difference in behavior of the higher and lower members of the Balmer series (Greenstein and Kraft 1959; Kraft 1959).

#### V. THE MASS-LOSS RATE

From the previous section, it is not inconsistent to assume that the mass loss from Z Cam is continuous and constant in time, and that the velocity of outflow is radial and constant throughout the shell. The equation of continuity then requires that the number density of hydrogen have the form

$$n_{\text{H}} = \frac{n_0(\theta, \phi)}{r^2}, \quad (2)$$

where  $r$  is the distance from the center of the shell. For a uniform conical shell, we have  $n_0$  independent of  $\phi$ ;  $n_0$  equals zero for  $60^\circ < \theta < 120^\circ$ ; and  $n_0$  is constant elsewhere, and equals  $k$ .

The  $H\alpha$  emission is a result of capture and cascade to the  $n = 3$  level of hydrogen. Since the physical conditions within the shell cannot be specified by the observations, we shall adopt those physical conditions which will tend to minimize the calculated rate of mass loss. The mass-loss rate is minimized if the shell is optically thick to Lyman lines, and optically thin to Balmer lines. This is case B of Baker and Menzel (1938). With these conditions, every effective recombination to the  $n = 3$  level eventually results in an  $H\alpha$  photon which escapes. Then energy given off by the shell in  $H\alpha$  is then

$$E_{3,2} = h\nu \int n_e n_i \alpha_3(T) dV, \quad (3)$$

where  $\alpha_3(T)$  is the total effective recombination coefficient to the  $n = 3$  level, and is temperature dependent. The number densities of electrons and hydrogen ions are  $n_e$  and  $n_i$ ,  $\nu$  is the frequency of an  $H\alpha$  photon, and the integration is carried out over the volume of the shell. If the shell is completely ionized, we have  $n_e \simeq n_i = n_{\text{H}}$ . Since  $\alpha_3(T)$  is only weakly dependent on temperature in the range  $10^3 \leq T \leq 10^5$  K, we shall assume that it is constant throughout the shell. Equation (3) becomes

$$E_{3,2} = 2\alpha_3(T)h\nu k^2 \int_{\phi=0}^{2\pi} \int_{\theta=0}^{\pi/3} \int_{R_1}^{\infty} \frac{\sin \theta dr d\theta d\phi}{r^2} \quad (4)$$

$$= \frac{2\pi\alpha_3(T)h\nu k^2}{R_1}, \quad (5)$$

where  $R_1$  is the inner radius of the shell. The rate of mass loss is given by

$$\frac{dM}{dt} = \frac{2m_{\text{H}}v_{\text{E}}k}{X_{\text{H}}} \int_{\phi=0}^{2\pi} \int_{\theta=0}^{\pi/3} \sin \theta d\theta d\phi \quad (6)$$

$$= \frac{2\pi m_{\text{H}}v_{\text{E}}k}{X_{\text{H}}}, \quad (7)$$

where  $m_{\text{H}}$  is the mass of a hydrogen atom, and  $X_{\text{H}}$  is the fraction of the mass due to hydrogen. Eliminating  $k$  between equations (7) and (5) we have finally

$$\frac{dM}{dt} = \frac{m_{\text{H}}v_{\text{E}}}{X_{\text{H}}} \left( \frac{2\pi R_1 E_{3,2}}{\alpha_3(T) h\nu} \right)^{1/2}. \quad (8)$$

We shall take  $R_1$  as twice the radius of the orbit of the G star which, from KKM and with an inclination of  $60^\circ$ , is  $1.8 \times 10^{11}$  cm. Taking the temperature of the shell to be  $10^4$  ° K, we find  $\alpha_3(10^4 \text{ ° K}) = 1.18 \times 10^{-13} \text{ cm}^3 \text{ s}^{-1}$  (Pengelly 1964). We shall adopt  $X_{\text{H}} = 0.7$ .

The contribution of the fine structure to the  $\text{H}\alpha$  profile is about 2 Å equivalent width (continuum = 1.00), or less than 0.1 of the total  $\text{H}\alpha$  equivalent width. The continuum is a sum of contributions from the G star and from the gas complex in the Roche lobe of the white dwarf. KKM note that the G spectrum is heavily and often completely veiled, so that the G star cannot contribute more than one-half of the continuum energy. Therefore, in terms of the G-star continuum, the fine structure has an equivalent width of at least 4 Å. Using the solar irradiance at 6550 Å from Labs and Neckel (1968) to calibrate the G continuum of Z Cam, the total  $\text{H}\alpha$  emission energy from the shell is  $E_{3,2} = 1.7 \times 10^{30} \text{ ergs s}^{-1}$ .

With the above parameters, the rate of mass loss is  $dM/dt = 2.4 \times 10^{-9} M_{\odot} \text{ yr}^{-1}$ . We emphasize that this rate of mass loss should be considered a lower limit.

Robinson (1973a) has calculated a strict lower limit to the rate of mass transfer in Z Cam of  $3.3 \times 10^{-9} M_{\odot} \text{ yr}^{-1}$ . Thus the lower limits to the rates of mass transfer and of mass loss are comparable. The relation of the lower limits to the true rates are uncertain, so that anywhere from a small fraction to nearly all of the mass which is transferred may also be lost from the system. We suggest that nearly all of the transferred mass is lost. Z Cam is the prototype of a small group of the dwarf novae showing occasional standstills on the descending slopes of their eruption light-curves. During standstill, the visual magnitude of Z Cam is about 11.5, which is about 1 mag fainter than the magnitude of Z Cam at the peak of an eruption. The standstills of Z Cam may last up to several years and appear to represent a steady-state condition for Z Cam. Lortet (1968) has found that the mean luminosity of Z Cam when averaged over its eruption light cycle is very close to its luminosity during standstill. If, as usual, we assume that the eruptions of Z Cam are due to the explosive detonation of the hydrogen-rich material which has accreted onto the white dwarf between eruptions, then we tentatively identify the standstill as the state in which the accreted matter is burned steadily as it is accreted. Estimating the visual magnitude of the G star in Z Cam to be about 14.5, and estimating the bolometric correction for the white dwarf during standstill to be 0.5 mag, we find the luminosity of Z Cam during standstill to be about  $25 L_{\odot}$  or  $10^{35} \text{ ergs s}^{-1}$ . Since burning 1 gram of stellar material liberates about  $9 \times 10^{18} \text{ ergs}$ , the white dwarf in Z Cam is burning mass at a rate of about  $1.7 \times 10^{-10} M_{\odot} \text{ yr}^{-1}$ . This is over an order of magnitude less than the absolute minimum mass-transfer rate of Z Cam. It appears, then, that of the mass which is transferred, over 90 percent is lost from the system before reaching the surface of the white dwarf.

In conclusion, we note that the effect of mass loss on the evolution of Z Cam is probably significant. Even if it is ultimately decided that much less than 90 percent of the transferred mass is subsequently lost from the system, the effects of non-conservation of mass and angular momentum may still have serious effects, so that studies of the evolution of Z Cam, and the dwarf novae in general (e.g., Faulkner 1971), may need to be reinterpreted.

This investigation was made during the author's tenure as the Benfield scholar, and the author gratefully acknowledges support from the David Benfield Memorial Fellowship Fund.

## REFERENCES

- Baker, J. G., and Menzel, D. H. 1938, *Ap. J.*, **88**, 52.  
 Elvey, C. T., and Babcock, H. W. 1943, *Ap. J.*, **97**, 412.  
 Faulkner, J. 1971, *Ap. J. (Letters)*, **170**, L99.  
 Gordelatse, S. G. 1938, *Bull. Abastumansk. Obs.*, **3**, 91.  
 Greenstein, J. L. 1960, in *Stars and Stellar Systems*, Vol. 6, *Stellar Atmospheres*, ed. J. L. Greenstein (Chicago: University of Chicago Press), p. 676.  
 Greenstein, J. L., and Kraft, R. P. 1959, *Ap. J.*, **130**, 99.  
 Herbig, G. H. 1960, *Ap. J.*, **132**, 76.  
 Huang, Su-Shu. 1972, *Ap. J.*, **171**, 549.  
 Hutchings, J. B. 1972, *M.N.R.A.S.*, **158**, 177.  
 Kraft, R. P. 1959, *Ap. J.*, **130**, 110.  
 ———. 1962, *ibid.*, **135**, 408.  
 ———. 1963, *Adv. Astr. and Ap.*, **2**, 43.  
 Kraft, R. P., Krzeminski, W., and Mumford, G. S. 1969, *Ap. J.*, **158**, 589 (KKM).  
 Krzeminski, W. 1965, *Ap. J.*, **142**, 1051.  
 Labs, D., and Neckel, H. 1968, *Zs. f. Ap.*, **69**, 1.  
 Lortet, M.-C. 1968, *Non-Periodic Phenomena in Variable Stars*, ed. L. Detre (Budapest: Academic Press), p. 381.  
 Mayall, M. W. 1965, *J.R.A.S. Canada*, **59**, 285.  
 Paczyński, B., Piotrowski, S., and Turski, W. 1968, *Ap. and Space Sci.*, **2**, 254.  
 Payne-Gaposchkin, C. 1957, *The Galactic Novae* (Amsterdam: North-Holland), chap. 3.  
 Pengelly, R. M. 1964, *M.N.R.A.S.*, **127**, 145.  
 Robinson, E. L. 1973a, *Ap. J.*, **180**, 121.  
 ———. 1973b, *ibid.*, in press.  
 Smak, J. 1969, *Acta Astr.*, **19**, 155.  
 ———. 1970, *ibid.*, **20**, 311.  
 ———. 1971, *ibid.*, **21**, 15.  
 Walker, M. F., and Chincarini, G. 1968, *Ap. J.*, **154**, 157.  
 Walker, M. F., and Reagan, G. H. 1971, *Information Bull. Var. Stars*, IAU Comm. No. 27, No. 544.  
 Warner, B., and Robinson, E. L. 1972, *Nature Phys. Sci.*, **239**, 2.